MOLECULAR AND CELLULAR BIOLOGY, Aug. 1997, p. 4611–4621 Vol. 17, No. 8
0270-7306/97/$04.00+0

Modulation of the Fate of Cytoplasmic mRNA by AU-Rich Elements: Key Sequence Features Controlling mRNA Deadenylation and Decay

NIANHUA XU, CHYI-YING A. CHEN, AND ANN-BIN SHYU*

Department of Biochemistry and Molecular Biology, The University of Texas Houston Health Science Center, Medical School, Houston, Texas 77030

Received 7 February 1997/Returned for modification 4 April 1997/Accepted 14 May 1997

Regulation of cytoplasmic deadenylation has a direct impact on the fate of mRNA and, consequently, its expression in the cytoplasm. AU-rich elements (AREs) found in the 3′ untranslated regions of many labile mRNAs are the most common RNA-destabilizing elements known in mammalian cells. AREs direct accelerated deadenylation as the first step in mRNA turnover. Recently we have proposed that AREs can be divided into three different classes. mRNAs bearing either the class I AUUUA-containing ARE or the class III non-AUUUA ARE display synchronous poly(A) shortening, whereas class II ARE-containing mRNAs are deadenylated asynchronously, with the formation of poly(A)$^-$ intermediates. In this study, we have systematically characterized the deadenylation kinetics displayed by various AREs and their mutant derivatives. We find that a cluster of five or six copies of AUUUA motifs in close proximity forming various degrees of reiteration is the key feature that dictates the choice between processive versus distributive deadenylation. An AU-rich region 20 to 30 nucleotides long immediately 5′ to this cluster of AUUUA motifs can greatly enhance the destabilizing ability of the AUUUA cluster and is, therefore, an integral part of the class I and class II AREs. These two features are the defining characteristics of class II AREs. Our results are consistent with the interpretation that the pentanucleotide AUUUA, rather than the nonamer UUAUUUA(U/A)(U/A), is both an essential and the minimal sequence motif of AREs. Our study provides the groundwork for future characterization of ARE-binding proteins identified by in vitro gel shift assays in order to stringently define their potential role in the ARE-mediated decay pathway. Moreover, transformation of deadenylation kinetics from one type to the other by mutations of AREs implies the existence of cross talk between the ARE and 3′ poly(A) tail, which dictates the decay kinetics.

Regulation of mRNA turnover is now recognized as an important mechanism for controlling the fate of cytoplasmic mRNA and, consequently, gene expression. The stability of mRNA can be modulated by specific *cis*-acting elements within mRNAs and their cognate *trans*-acting factors (3, 13, 24). Adenylate- and uridylate-rich (AU-rich) elements (AREs) found in the 3′ untranslated regions (UTRs) of many highly unstable mRNAs represent thus far the most common RNA stability determinant among those characterized in mammalian cells (7). Based on their sequence features and functional properties, recently we proposed that AREs can be divided into at least three classes (7, 22). Class I and class II AREs contain various copies of an AUUUA motif, whereas class III AREs do not bear this pentanucleotide. AREs classified as class I are mostly found in early-response-gene mRNAs that encode nuclear transcription factors (6, 7) and also in mRNAs for some cytokines, such as interleukin 4 (IL-4) and IL-6 (4, 25). They contain one to three copies of dispersed AUUUA motifs coupled with nearby U-rich sequences or U stretches. Mutagenesis experiments with the c-*fos* ARE indicated that each of these sequence features plays a distinct role within the class I ARE and together they determine the final destabilizing potency of the class I ARE (5). It is interesting that so far AREs assigned to class II are all from cytokine mRNAs, e.g., the granulocyte-macrophage colony-stimulating factor (GM-CSF) ARE, tumor necrosis factor alpha (TNF-α) ARE, and IL-3 ARE, and have multiple copies of AUUUA pentanucleotides that cluster together (see Fig. 1).

The three different classes of AREs appear to direct rapid mRNA decay with two distinct kinetics (7) (see Fig. 2). The GM-CSF ARE, a representative of the class II AREs, directs asynchronous cytoplasmic deadenylation with the appearance of a smear that ends at the poly(A)$^-$ position (see Fig. 3A). The formation of these kinetic intermediates, with the smallest one being poly(A)$^-$, is consistent with a processive ribonucleolytic digestion of poly(A) tails (8). In contrast, class I AUUUA-containing AREs, e.g., the c-*fos* ARE, and class III non-AUUUA AREs, such as the c-*jun* ARE, mediate synchronous poly(A) shortening followed by the decay of mRNA body, indicating that ribonucleolytic digestion of poly(A) tails is a result of distributive enzymatic action (see Fig. 2 and 3A). Therefore, mRNAs carrying either class I or class III AREs exhibit a biphasic decay pattern, as detected by high-resolution Northern blotting. During the first phase, all the mRNA molecules appear to undergo a similar rate of deadenylation with little or no degradation. In the second phase, poly(A) shortened mRNAs are then quickly degraded. Since regulation of cytoplasmic deadenylation has been shown to have a profound effect on the fate of mRNA (13, 14, 23), it becomes critical to elucidate the key sequence features that specify the two distinct types of cytoplasmic deadenylation.

Two recent studies have shown that synthetic AREs, consisting of different copies of the nonamer UUAUUUA(U/A)(U/A) with the AUUUA core, are able to confer various de-

* Corresponding author. Phone: (713) 500-6068. Fax: (713) 500-0652.

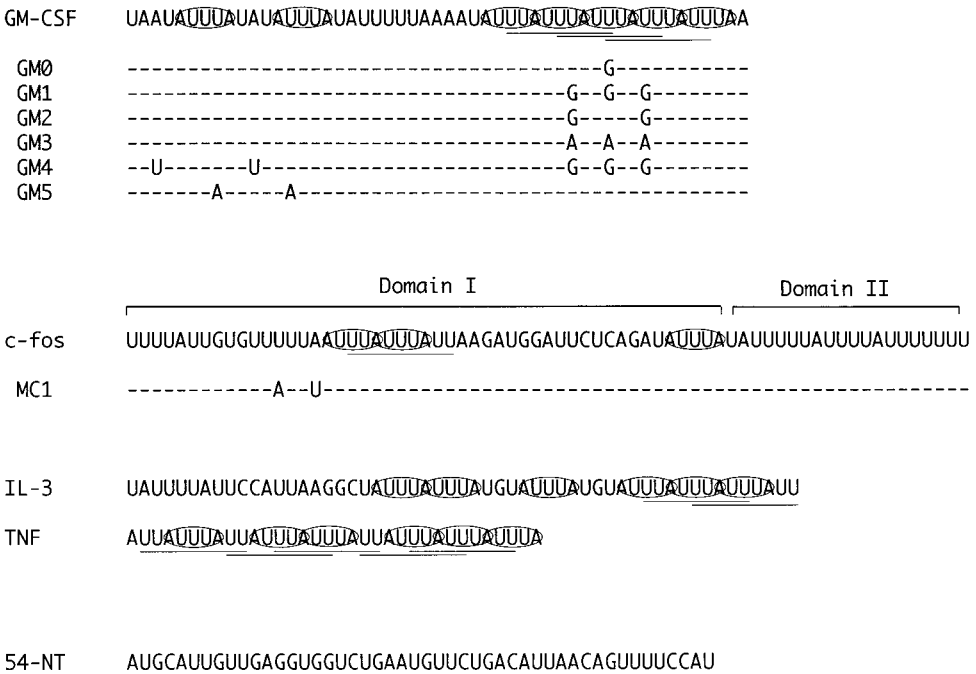

FIG. 1. RNA sequences of AREs, their mutant derivatives, and a 54-nt AU-rich region. The sequence of each ARE is listed. In mutant AREs, the mutated nucleotides are shown, while the unchanged nucleotides are indicated by dashes. The AUUUA motifs are circled, and the nonamers are underlined. c-*fos* ARE is composed of two domains, domain I and domain II (5). TNF, TNF-α; 54-NT, 54-nt AU-rich region.

grees of destabilization on otherwise stable reporter messages (15, 33). Interestingly, reiteration or clustering of AUUUA motifs concomitantly gives rise to an RNA sequence with overlapping UUAUUUAUU nonamers, which we had previously proposed to be a characteristic of the class II AREs (7, 22). Based on these observations, we had tentatively concluded that the existence of overlapping nonamers leads to asynchronous deadenylation kinetics (7). However, it is unclear whether the mere presence, copy number, position and/or overlapping nature of the nonamers is required for a class II AUUUA-containing ARE to exert its destabilizing function. In addition, it also remains to be determined whether sequences other than that of the nonamers may be necessary for the class II ARE to obtain its full destabilizing function. Finally and more importantly, is it the clustering of AUUUA motifs in close vicinity or the overlapping nature of nonamers that represents the entity recognized by the decay machinery in the class II ARE?

In this study we have examined several class II-like AREs and carried out extensive and systematic site-directed mutagenesis of AREs from both class I and class II AUUUA-containing AREs. Destabilizing functions and decay kinetics of these AREs were fully examined by performing time course experiments using the c-*fos* serum-inducible promoter system (26, 28, 31). These experiments allowed us to gain in-depth understanding of the key sequence features in AREs that control the rates and kinetics of cytoplasmic deadenylation. They also led to the identification of characteristics of the class II AREs and further support our classification of AREs. Our characterizations of the sequence features of AREs will provide the groundwork for future investigation of ARE-binding proteins, whose cDNAs have been cloned (11, 16, 17, 19–21, 32), in order to stringently define their participation in the ARE-mediated mRNA degradation.

MATERIALS AND METHODS

Cell culture and DNA transfection. Mouse NIH 3T3 cells were cultured in Dulbecco's modified Eagle's medium (DMEM) with 10% calf serum (CS; Gibco). Cells were split to 2×10^6 per 100-mm-diameter dish 16 to 20 h prior to transfection by the calcium phosphate technique, as described previously (27). At 16 h after transfection, cells were washed twice with phosphate-buffered saline and serum starved in DMEM with 0.5% CS for 25 h prior to stimulation with DMEM with 20% CS, as described previously (27).

Plasmid construction. The construction of plasmids pBBB+ARE$^{c\text{-}fos}$, pBBB+ARE$^{GM\text{-}CSF}$, and pSVα1-GAPDH has been described previously (5, 6, 8, 28). Mutant c-*fos* and GM-CSF AREs were generated by standard PCR-mediated site-directed mutagenesis (12) using either pBBB+ARE$^{c\text{-}fos}$ or pBBB+ARE$^{GM\text{-}CSF}$ as the template. Oligonucleotide primers carrying mutations and restriction enzyme sites were custom synthesized from Genosys (Woodland, Tex.). Sequences of mutant AREs are shown in Fig. 1. The PCR-amplified fragment containing mutant ARE GM0, GM1, GM2, or GM3 was flanked by an *Eco*RI site at the 5′ end and a *Bgl*II site at the 3′ end. After *Eco*RI and *Bgl*II digestion, the PCR-amplified fragment was used to replace the corresponding fragment cut out from pBBB by *Eco*RI and *Bgl*II. The PCR-amplified fragment containing the GM4, GM5, or MC1 ARE was flanked by a *Bam*HI site at the 5′ end and a *Bgl*II site at the 3′ end. Following *Bam*HI and *Bgl*II digestion, the PCR-amplified fragment was inserted into the unique *Bgl*II site in pBBB.

To construct pBBB+ARE$^{IL\text{-}3}$, a pair of oligomers that share a 9-nucleotide (nt) complementary region were synthesized (5′-CGGGATCCTATTTTATTCCATTAAGG-3′, 5′-GAAGATCTAATAAATAAATAAATACATAAATACATAAATAAATAGCCTTAATGG-3′). After the sequences annealed to each other, Klenow polymerization reaction was performed to make double-stranded DNA which was flanked by a *Bam*HI site at the 5′ end and a *Bgl*II site at the 3′ end. The DNA fragment was digested with these enzymes and was then subcloned into pBBB at its unique *Bgl*II site. To construct pBBB+ARE$^{TNF\text{-}\alpha}$, a pair of complementary 38-mers were synthesized (5′-GATCATTATTTATTATTTATTATTTATTTATTTATTA-3′, 5′-GATCTAAATAAATAAATAATAAATAAATAATAAATAAT-3′). After the sequences were annealed to each other, the double-stranded DNA fragment was flanked by 5′-GATC protruding termini and was directly subcloned into pBBB at its unique *Bgl*II site. The sequences of ARE$^{IL\text{-}3}$ and ARE$^{TNF\text{-}\alpha}$ are shown in Fig. 1.

To create plasmid pBBB^{54}, a 134-bp region in plasmid pBBB132 (26) spanning the last 80 bp of the carboxyl-terminal region of the rabbit β-globin gene and the 54-bp region immediately upstream of the human c-*fos* ARE was amplified by standard PCR techniques. The PCR product was digested with *Eco*RI and *Bgl*II and was subsequently subcloned between the *Eco*RI and *Bgl*II sites of plasmid pBBB. The resulting plasmid contains at its unique *Bgl*II site the 54-bp region

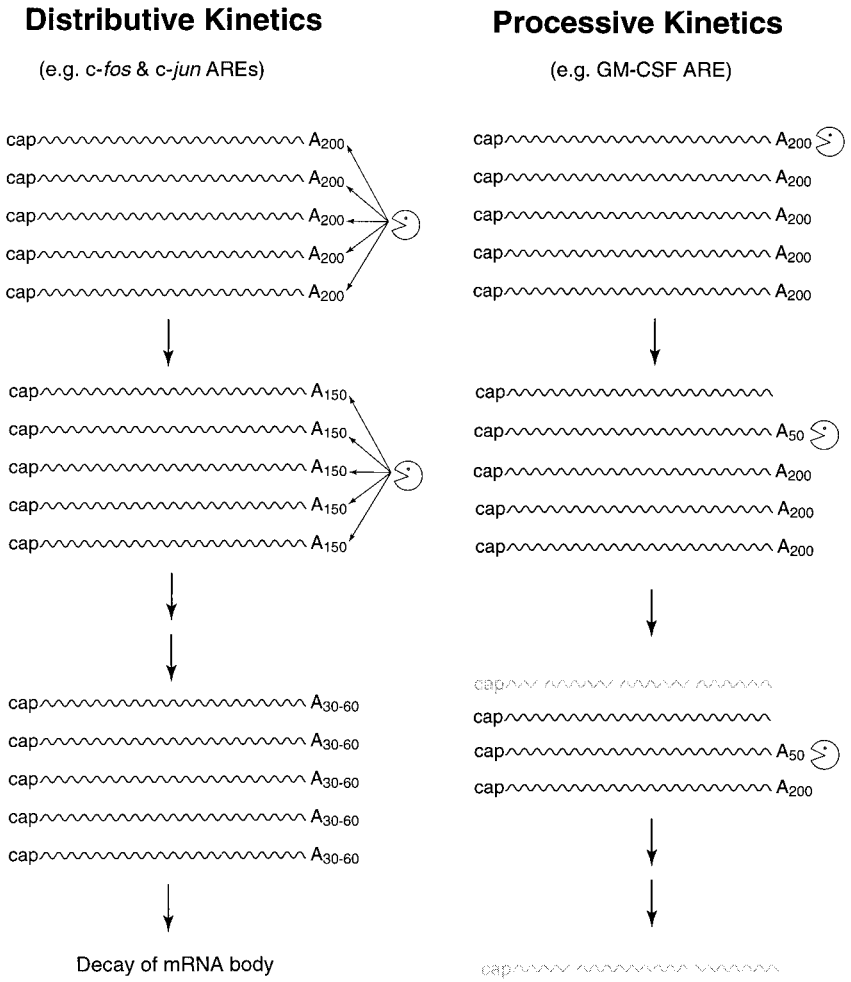

FIG. 2. A general model showing two distinct deadenylation and decay kinetics displayed by the three classes of AREs. (Left) For decay mediated by the class I AUUUA-containing ARE and the class III non-AUUUA ARE, the mRNA population undergoes synchronous poly(A) shortening and is deadenylated at a similar rate, implying the action of a distributive ribonucleolytic digestion of poly(A) tails. Synchronous removal of poly(A) tails to a size of 30 to 60 nt, during which period the mRNA concentration remains fairly constant, is followed by rapid degradation of mRNA body. (Right) The population of class II AUUUA-containing ARE mRNAs is deadenylated asynchronously, with the formation of kinetic intermediates that include fully deadenylated species, consistent with the action of a processive ribonucleolytic digestion of poly(A) tails. Asynchronous poly(A) shortening to poly(A)$^-$ species parallels the immediate and rapid degradation of transcribed mRNA body. Pacman, RNase or RNase complex; solid wavy line, mRNA body; gray stippled wavy line, degraded mRNA body.

(Fig. 2). ARE^{GM4}, ARE^{MC1}, and ARE$^{TNF\text{-}\alpha}$ were then subcloned into pBBB^{54} at the unique *Bgl*II site which is now located immediately downstream of the 54-bp region to create 54GM4, 54MC1, and 54TNF, respectively.

To construct pBBB^{NSC}, a nonsense codon was created by a C-to-T change in the last exon of the β-globin gene in pBBB. The mutation is located 65 nt upstream of the normal translation stop codon. Briefly, the sense strand oligomer (5′-GCAAAGAATTCACTCCTTAGGTGCAGGCTGCC-3′) carries the translational premature termination mutation and an *Eco*RI site at its 5′ end. The antisense primer (5′-CCGGTGCGCAATTGCAATGAAAAT-3′) is complementary to the 24-bp region immediately upstream of the poly(A) addition site. The PCR product was cut with *Eco*RI and *Bgl*II and swapped with the corresponding fragment cut out from pBBB by the same pair of enzymes. Likewise, the plasmids bearing both the nonsense codon and mutant ARE, such as pBBB^{NSC}+ARE^{MC1}, pBBB^{NSC}+ARE^{GM4}, and pBBB^{NSC}+ARE$^{TNF\text{-}\alpha}$, were constructed in a similar way except that antisense primers complementary to different AREs were used in the PCR amplification to amplify the region between *Eco*RI and *Bgl*II sites in corresponding pBBB+ARE plasmids. The syn1 ARE was created from a pair of complementary 22-mers (GATCTTATTTATT TATTTATTA; GATCTAATAAATAAATAAATAA). After the sequences were annealed to each other, the double-stranded DNA fragment was flanked by 5′-GATC protruding termini and was directly subcloned into the unique *Bgl*II site of plasmid pBBB or pBBB^{54} to generate pBBB+ARE^{syn1} or pBBB+ARE^{syn2}, respectively. DNA sequencing was performed to confirm all of the AREs and their mutant constructs.

Analysis of mRNA decay and deadenylation. Total cytoplasmic RNAs were isolated at various times after serum stimulation of transiently transfected NIH 3T3 cells. RNase H treatment of cytoplasmic mRNA was carried out to generate poly(A)$^-$ RNA (26), and mRNA decay and deadenylation were analyzed by Northern (RNA) blot analysis as described previously (26). Electrophoresis was done on 1.4% formaldehyde-agarose gels. A 123-bp DNA ladder (Gibco) was denatured and included to provide a molecular size standard. The amount of specific mRNA was quantitated directly by scanning blots on an imager (Packard) and normalized with respect to the hybrid alpha-globin/glyceraldehyde-3-phosphate dehydrogenase (α/GAPDH) internal standard.

RESULTS

Clustering of AUUUA motifs or overlapping of UUAUUUA (U/A)(U/A) nonamers leads to asynchronous deadenylation kinetics. To address the potential role of the clustering of AUUUA motifs (or the overlapping of nonamers) in class II ARE-direct mRNA decay, we first examined the deadenylation kinetics of AREs with sequence features similar to those of the GM-CSF ARE. GM-CSF ARE is the representative of the class II AREs. mRNAs bearing it undergo asynchronous deadenylation (Fig. 3A). In addition to two scattered copies of the AUUUA motifs, the GM-CSF ARE contains at its 3′ end five AUUUA motifs that group together to give the sequence

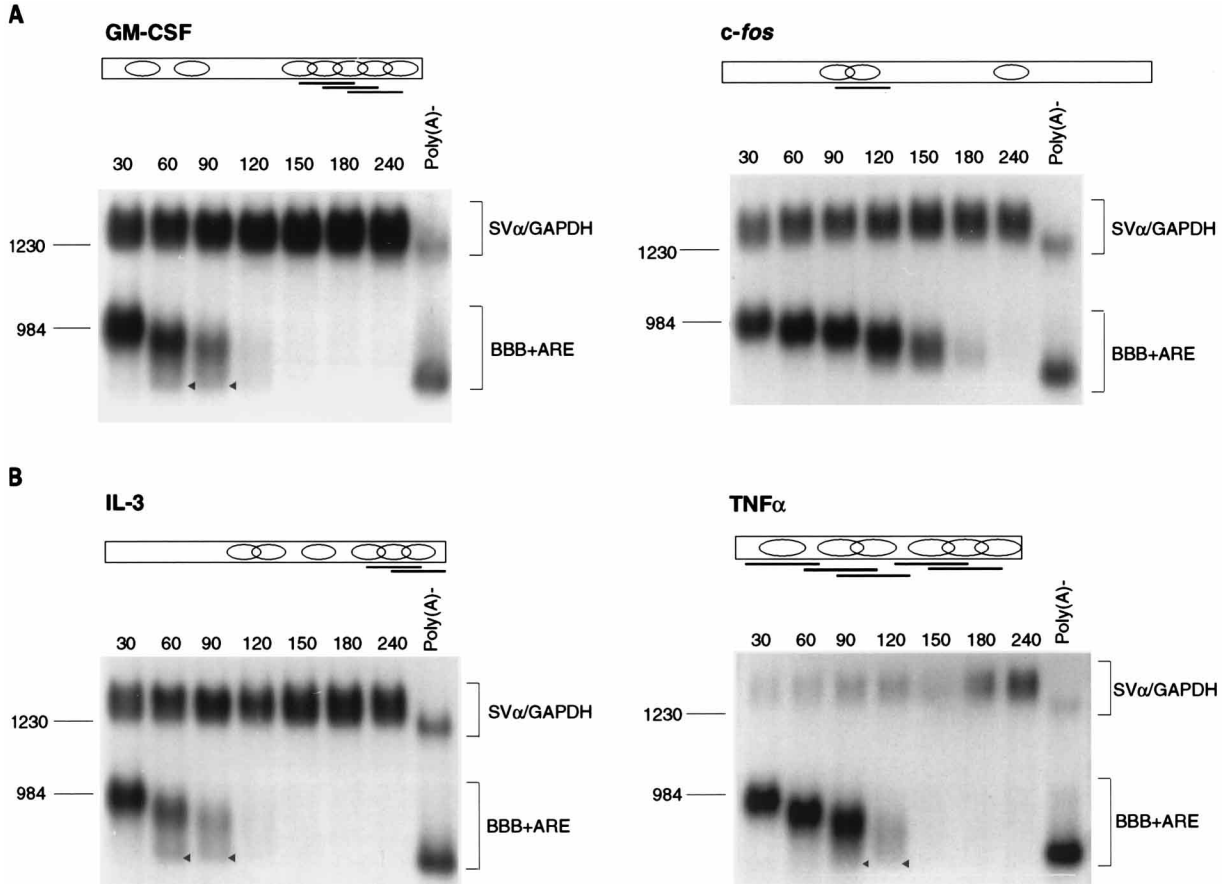

FIG. 3. β-Globin mRNA bearing the IL-3 ARE or TNF-α ARE deadenylates and decays with kinetics similar to that of the GM-CSF ARE. NIH 3T3 cells were transiently cotransfected with the control plasmid pSVα1/GAPDH and one of the test plasmids. Total cytoplasmic mRNA was isolated at various time intervals after serum stimulation and analyzed by Northern blot analysis. SVα1/GAPDH mRNA was constitutively expressed and served as an internal standard for normalizing variations from transfection efficiency and sample handling. (A) Northern blots showing the mRNA decay of BBB+ARE$^{GM\text{-}CSF}$ (left) and BBB+ARE$^{c\text{-}fos}$ (right). (B) Northern blots showing the mRNA decay of BBB+ARE$^{IL\text{-}3}$ (left) and BBB+ARE$^{TNF\text{-}\alpha}$ (right). The times given on the top correspond to minutes after serum addition. Thirty minutes after serum stimulation, BBB+ARE mRNAs all retained a full-length poly(A) tail (~200 nt). Poly(A)$^-$ RNA was prepared in vitro by treating RNA samples from the 30-min time point with oligo(dT) and RNase H. Seen in the decay of BBB+ARE$^{GM\text{-}CSF}$, BBB+ARE$^{IL\text{-}3}$, and BBB+ARE$^{TNF\text{-}\alpha}$ mRNAs is the presence of a smear underneath the major band with its bottom edge (solid triangles) corresponding to poly(A)$^-$ species. This is consistent with the interpretation that poly(A) tails are processively removed. The 123-bp DNA ladder from Gibco BRL was used as molecular size standards. The positions corresponding to 1230 and 984 nt are indicated. Schematic drawings of AREs are shown over the blots. In the schematic drawings, an open rectangle represents an ARE, open ovals inside the rectangle represent the AUUUA motifs, and thin black bars under the rectangle represent the nonamers.

$(AUUU)_5A$. This sequence concomitantly gives rise to three overlapping UUAUUUAUU nonamers (Fig. 1). Two AREs were selected, one from the 3′ UTR of IL-3 and the other from the 3′ UTR of TNF-α (Fig. 1). The IL-3 ARE has six AUUUA motifs that also cluster at the 3′ portion. In addition, three of the six copies give rise to two overlapping nonamers. Likewise, the TNF-α ARE has six AUUUA motifs that cluster together and result in five nonamers overlapping with each other throughout the entire ARE.

Destabilizing functions of these two AREs were determined by inserting them into the 3′ UTR of the stable β-globin mRNA. Transient expression of these chimeric messages was driven by the serum-inducible c-*fos* promoter (10, 30). Plasmids carrying the chimeric genes were introduced individually into NIH 3T3 cells by transient cotransfection with a control plasmid, from which a control mRNA, designated α/GAPDH, was constitutively expressed. The control message served as an internal standard to correct for variations in transfection efficiency and sample handling. Transcription of the chimeric genes from the c-*fos* promoter was transiently induced by stimulation of quiescent NIH 3T3 cells with 20% CS. Total cytoplasmic mRNA was isolated at time intervals and analyzed by Northern blotting (see Materials and Methods for experimental details).

The results showed that the deadenylation and decay kinetics displayed by the IL-3 ARE are indistinguishable from those of the GM-CSF ARE (Fig. 3B). The chimeric mRNAs bearing the IL-3 ARE underwent asynchronous deadenylation with the appearance at the 60-min time point of a smear ending at the poly(A)$^-$ position (Fig. 3). Like the GM-CSF ARE, the IL-3 ARE reduced the half-life of the stable β-globin mRNA from greater than 10 h down to ~22 min (Table 1). The TNF-α ARE-directed decay also showed similar decay and deadenylation kinetics, albeit slightly retarded (Fig. 3B). Deadenylation of BBB+ARE$^{TNF\text{-}\alpha}$ mRNAs became asynchronous at the 90-min time point with the appearance of the smear, which coincided with the onset of decay of RNA body. It reduced the half-life of β-globin mRNA down to ~28 min (Table 1). Together, these results substantiated our previous classification of the two AREs as class II AREs and suggested that clustering of AUUUA motifs or overlapping of nonamers represents a critical sequence feature that dictates the asynchronous deadeny-

TABLE 1. Effect of the clustering of AUUUA motifs on ARE destabilizing function

ARE	No. of AU_3A	Distribution of AU_3A motifs	No. of nonamers	$t_{1/2}$ (min)[a]	Fold stabilization[b]	Deadenylation kinetics[c]
GM-CSF	7	Clustered	3	21.4 ± 3.8	1.0	p
GM0	6	Clustered	0	24.5 ± 3.1	1.1	p
GM1	4	Dispersed	0	51.0 ± 3.3	2.4	d
GM2	5	Dispersed	0	37.9 ± 4.7	1.8	d
GM3	4	Dispersed	0	37.2 ± 6.7	1.7	d
GM4	5	Clustered	3	29.1 ± 2.2	1.4	Delayed p
GM5	5	Clustered	3	18.8 ± 3.4	0.8	p
c-*fos*	3	Dispersed	1	38.7 ± 3.0		d
MC1	4	Clustered	3	27.5 ± 3.0		Delayed p
IL-3	6	Clustered	2	21.7 ± 3.4		p
TNF-α	6	Clustered	5	28.3 ± 0.4		p
syn1	3	Clustered	3	135 ± 33		d

[a] $t_{1/2}$, half-life. Means ± standard deviations are shown. Standard deviations are derived from averaging the data from two independent experiments.
[b] Comparing $t_{1/2}$s of AREs to that of wt GM-CSF ARE.
[c] p, processive; d, distributive.

lation unique to the class II ARE. The slightly retarded kinetics seen in the TNF-α ARE-directed decay suggested that a feature(s) other than the cluster of AUUUA motifs in the GM-CSF and IL-3 AREs is also necessary for these two AREs to display the observed fully asynchronous deadenylation kinetics and faster decay kinetics.

The clustering of AUUUA motifs, rather than the overlapping of UUAUUUA(U/A)(U/A) nonamers, is the entity recognized by the decay machinery. The above results indicated that one of two factors, a cluster of five or six copies of AUUUA motifs or overlapping nonamers, plays a critical role in determining the unique decay kinetics of the class II ARE. Intriguingly, although the TNF-α ARE contains five nonamers, it is the least potent among the three class II AREs examined. On the other hand, the IL-3 ARE has only two nonamers, yet it is just as potent as the GM-CSF ARE, which contains three nonamers. These observations raise the issue of whether the nonamer consensus sequence represents a recognizable sequence motif. To address this point, we utilized mutagenesis of the GM-CSF ARE. A single-point mutation (GM0), a double-point mutation (GM2), and a triple-point (GM1) mutation (Fig. 1) were introduced into the GM-CSF ARE to knock out all three copies of the nonamers at once. The mutation in GM0 eliminated only one copy of the five AUUUA motifs and did not cause significant change in the clustering of AUUUA motifs. In contrast, mutations in GM1 and GM2 not only further reduced the copy number of the AUUUA motifs but also changed the five AUUUA motifs clustering at the 3′ portion of GM-CSF ARE into two and three dispersed AUUUA motifs, respectively. This made the GM1 and GM2 AREs resemble the class I AREs. Our prediction was that if the nonamers are critical, these mutant AREs lacking all three nonamers should exhibit the same phenotype. On the other hand, if the cluster of AUUUA motifs is important, then the stabilization effect should parallel the number and the way the AUUUA motifs are arranged.

As shown in Fig. 4, the deadenylation and decay directed by the GM0 ARE lacking any nonamers showed rather modest changes. The GM0 ARE remained able to direct rapid decay and deadenylation with kinetics similar to that of the TNF-α ARE, which contains five overlapping nonamers. Moreover, both GM1 and GM2 AREs also remained fairly potent and displayed a biphasic decay pattern, with synchronous deadenylation preceding decay of the RNA body, typical of class I AREs. These results clearly demonstrate that nonamers are dispensable and are not necessary for the destabilizing function of the GM-CSF ARE. They support the view that the cluster of five copies of AUUUA motifs is a key feature of the class II AREs. We interpreted the minor change in the deadenylation and decay pattern seen for GM0 to be the result of knocking out an AUUUA motif, which interrupts the continuity of AUUUA reiteration.

Since the mutation created in the GM1 or GM2 ARE also reduced the AU content and AU continuity in the 3′ portion of the GM-CSF ARE, we further tested the effects of these changes. Another GM-CSF ARE mutant (GM3 [Fig. 1]) was created by changing the U residues at the same positions as in GM1 to three A residues, thus maintaining both the AU percentage and AU continuity of the 3′ portion. Results in Fig. 4 showed that β-globin mRNA bearing the GM3 ARE decayed with kinetics similar to that containing the GM1 or GM2 ARE. More importantly, this result showed that the GM3 ARE, which also does not carry a copy of the nonamer, still retains potent destabilizing ability, further demonstrating that nonamers are dispensable. Taken together, these results provide strong evidence that it is the clustering of five or six copies of AUUUA motifs, rather than the overlapping of nonamers, which specifies the extraordinary rapid decay and asynchronous deadenylation seen in the class II AREs.

Modulation of deadenylation kinetics is achieved through mutation of *cis*-acting sequence features within the ARE. We next addressed whether the class I AREs can be transformed into class II AREs by introducing extra copies of the AUUUA motif into them so that a cluster of AUUUA motifs was generated. A double-point mutation was introduced at the 5′ portion of the c-*fos* ARE, a representative class I ARE, to create three AUUUA motifs reiterating with each other (MC1 [Fig. 1]). In addition, a double-point mutation was also introduced into the GM1 ARE to convert the two scattered AUUUA pentanucleotides at the 5′ portion of the GM1 ARE into three AUUUA motifs reiterating with each other (GM4 [Fig. 1]). Note that both AREs now contain at their 5′ portions three overlapping nonamers. As shown in Fig. 5A, decay of the β-globin mRNA carrying these mutant AREs began with synchronous deadenylation until the 90-min time point, after which the deadenylation pattern became asynchronous with the appearance of the smear at the 120-min time point and decay of the mRNA body occurred. The results showed that these manipulations can only partially transform the class I ARE into a class II-like ARE. They suggest that the modest

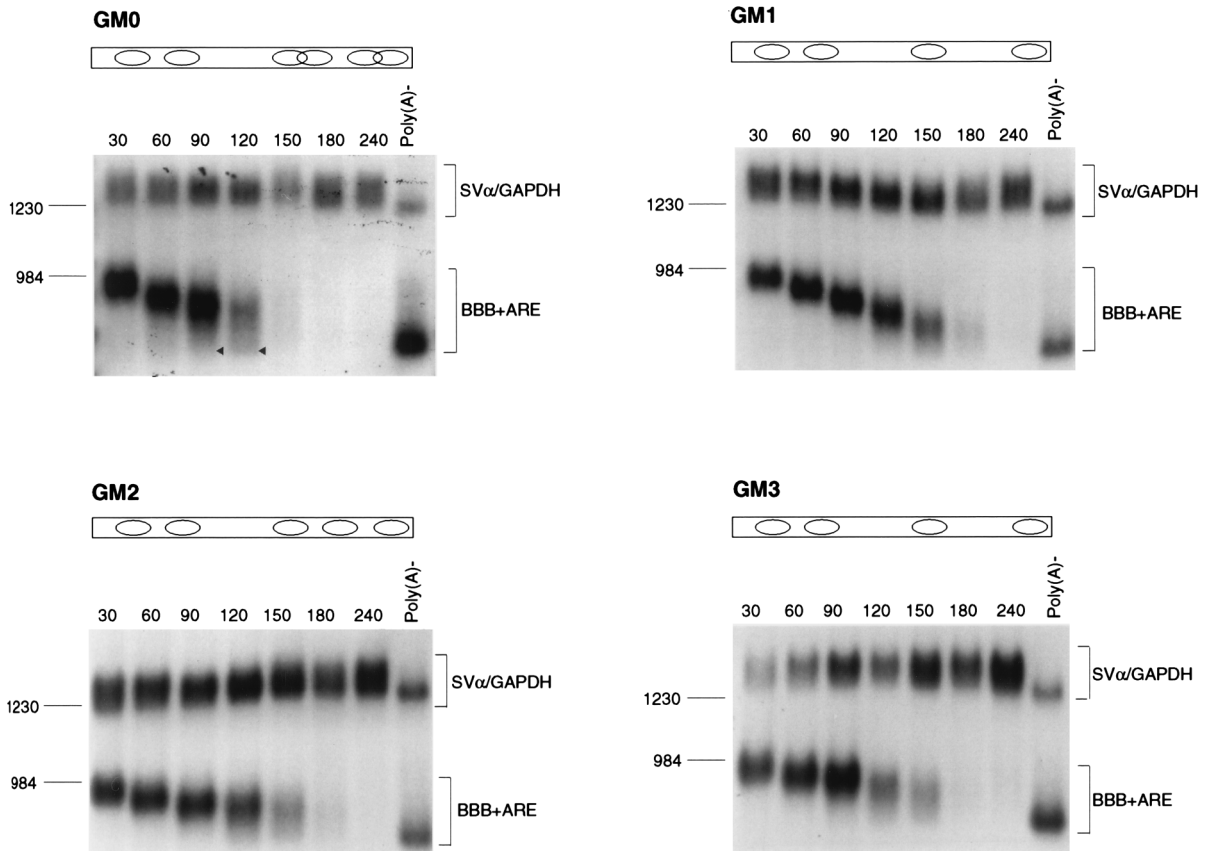

FIG. 4. Mutagenesis study of the GM-CSF ARE indicates that a cluster of AUUUA motifs, instead of the overlapping nonamers, is the key feature that specifies the decay pattern of mRNA carrying class II AREs. Northern blots showing deadenylation and decay of β-globin mRNAs bearing various mutant GM-CSF AREs. The schematic drawings of AREs, transient transfection, RNA isolation, and time course experiments are as described in the legend to Fig. 3. Note that all the point mutations knocking out overlapping nonamers only slightly retarded the decay.

reiteration of AUUUA motifs created in MC1 and GM4 AREs can enhance the asynchronous deadenylation and accelerate mRNA degradation, albeit at a somewhat slower rate than the wild-type (wt) GM-CSF ARE (Fig. 3A). These findings further indicated that features other than the cluster of AUUUA motifs are necessary to specify the full destabilizing ability characteristic of the GM-CSF and IL-3 AREs (see above).

A 5′ AU-rich region is also necessary for the full transformation of a class I ARE to a class II ARE. When comparing the destabilizing abilities of all the AREs that display class II-like decay kinetics, one interesting correlation was noticed. Clusterings of AUUUA motifs are found in the 3′ portions of the GM-CSF ARE and IL-3 ARE, which are 20 to 30 nt downstream from the 5′ ends of these AREs. Both AREs exhibit thus far the most potent destabilizing function. A similar clustering of AUUUA motifs seen in the less potent AREs, MC1 and GM4, is located in the 5′ portion of the ARE, 2 to 10 nt from its 5′ end (Fig. 1). The TNF-α ARE, which has a cluster of six AUUUA motifs but does not have any 5′-flanking region, also can only direct decay with kinetics similar to those of MC1 and GM4 (Fig. 3 and 5).

Since all the AREs we tested were inserted immediately downstream from the translation stop codon of the β-globin mRNA, one possibility was that in the cases of MC1, GM4, and TNF-α AREs, when translating ribosomes stop at the termination codon, they might impose some physical steric hindrance onto the AUUUA motifs that in turn interferes with their proper interaction with or recognition by the *trans*-acting factors. In contrast, the 20- to 30-nt sequence 5′ to the cluster of AUUUA motifs found in the GM-CSF and IL-3 AREs might provide a spacer to separate the cluster of AUUUA motifs from the translation stop codon. To gain further insight into this possibility, we introduced a premature termination codon in the carboxyl end of the protein-coding region located at the last exon of the β-globin gene so that a 65-nt region (42% AU content) between the nonsense codon and the original stop codon now became a nontranslated region that served as a spacer (Fig. 5B).

A time course experiment was first carried out to determine the stability of β-globin mRNA bearing this nonsense codon at the carboxyl end. The result in Fig. 5B showed that BBB^{NSC} remains as stable as the wt β-globin mRNA, demonstrating that the premature termination codon does not cause any unexpected destabilization of the stable β-globin mRNA. The MC1, GM4, and TNF-α AREs were then inserted immediately downstream of the newly created spacer region in the mutant β-globin gene. The destabilizing functions of these AREs were determined. As shown in Fig. 5B, none of these new chimeric mRNAs deadenylated and decayed with kinetics and stability similar to those mediated by the GM-CSF or IL-3 ARE. These results did not support the above possibility.

Since in GM-CSF and IL-3 AREs, the 20- to 30-nt regions upstream from the cluster of AUUUA motifs are relatively AU-rich, we next tested if an AU-rich region placed 5′ to the MC1, GM4, and TNF-α AREs is able to enhance their desta-

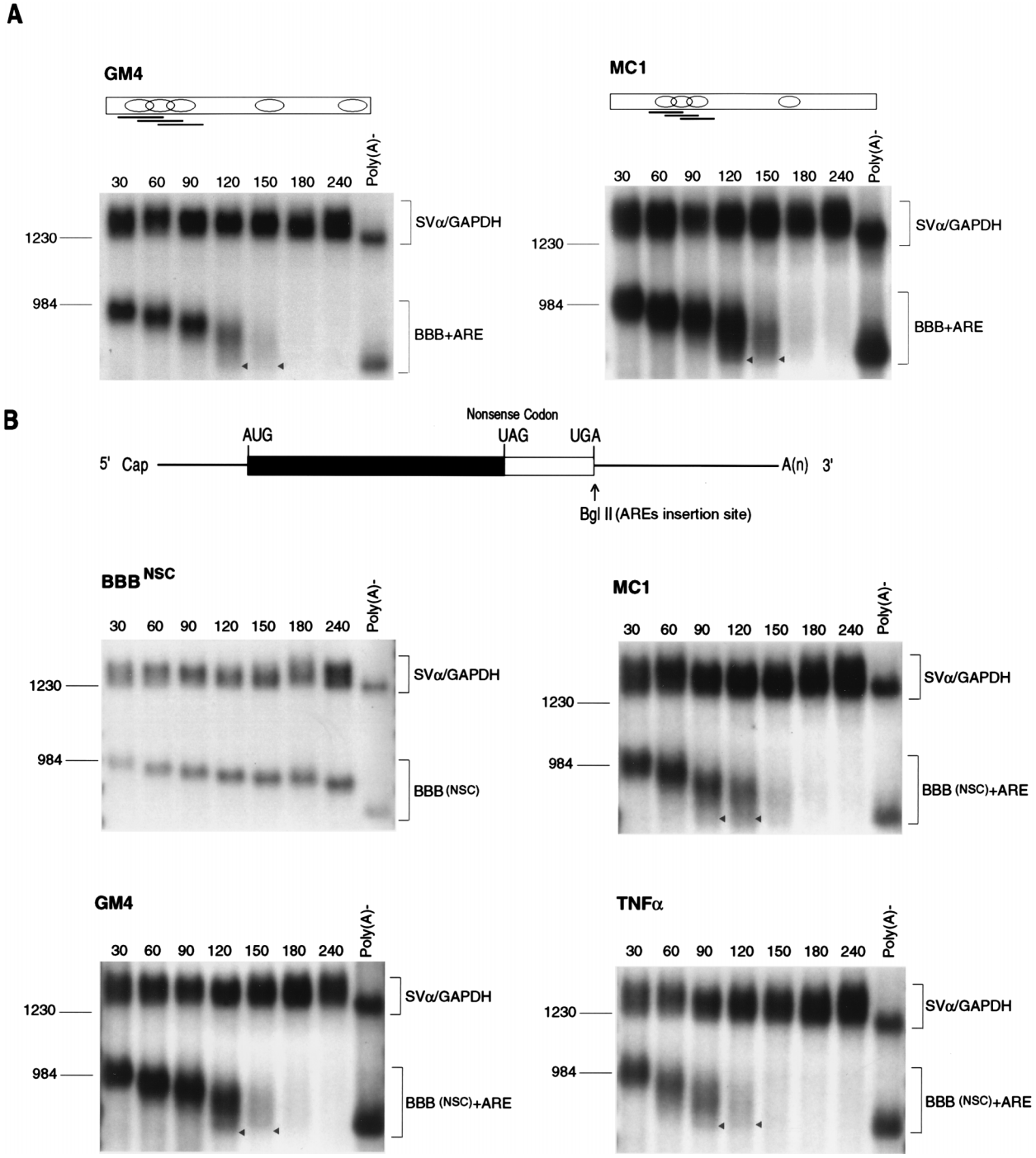

FIG. 5. Partial transformation of class I AREs into class II AREs cannot be achieved by merely increasing the space between the stop codon and the ARE. The schematic drawings of AREs, transient transfection, RNA isolation, and time course experiments are as described in the legend to Fig. 3. (A) Northern blots showing deadenylation and decay of β-globin mRNAs bearing GM4 and MC1 AREs. (B) The drawing at the top represents a schematic diagram of the β-globin mRNA bearing a nonsense codon (BBB^{NSC}). The solid box represents the coding region, and the adjacent open box represents the region that is no longer part of the open reading frame after the premature termination mutation. The nonsense codon is indicated at top, and the *Bgl*II site marks where AREs are inserted. The normal translation start and stop codons are also indicated. Northern blots show deadenylation and decay of BBB^{NSC} mRNAs bearing various AREs. The times given on the top correspond to minutes after serum addition.

bilizing power to a level comparable to those of the GM-CSF and IL-3 AREs. A 54-nt region with 62% AU content and without any AUUUA or nonamer motif (Fig. 1) was chosen from the c-*fos* 3′ UTR and was inserted into the immediate 5′ ends of the MC1, GM4, and TNF-α AREs. To ensure that the 54-nt sequence does not fortuitously possess any destabilizing function, we first introduced this sequence into the 3′ UTR of the wt β-globin mRNA. As shown in Fig. 6A, the BBB54 mRNA was as stable as the wt BBB mRNA, which displayed the same slow deadenylation. The effects of the 54-nt region on

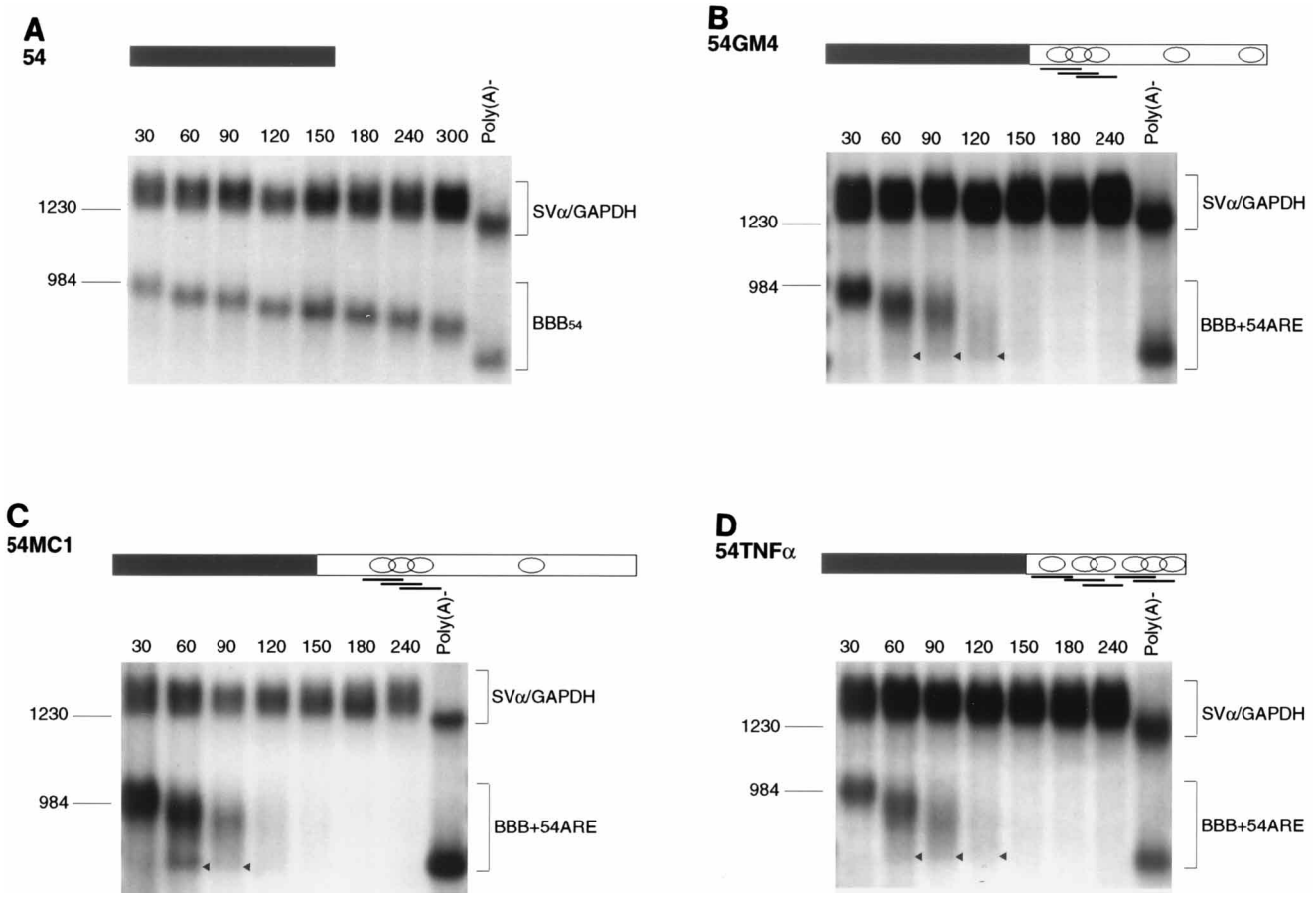

FIG. 6. The AU-rich region 5′ to the AUUUA cluster is an integral part of class II AREs. The schematic drawings of AREs, transient transfection, RNA isolation, and time course experiments are as described in the legend to Fig. 3. (A) Northern blot showing that the 54-nt AU-rich sequence itself (Fig. 1) does not cause any destabilization of the β-globin mRNA or change its deadenylation. β-Globin mRNA bearing the 54-nt AU-rich region decays slowly, with a half-life of more than 10 h, similar to that of wt β-globin mRNA. (B to D) The 54-nt AU-rich fragment enhances the destabilizing function of several class II-like AREs bearing a cluster of AUUUA motifs to a level equivalent to that of the wt GM-CSF ARE. The gray box adjacent to the ARE depicts the 54-nt AU-rich region, which is placed immediately upstream of the ARE. Please note that experiments in this figure were carried out in parallel with those testing GM4, MC1, and TNF-α AREs.

the destabilizing function of the MC1, GM4, and TNF-α AREs were then tested. As shown in Fig. 6B to D, insertion of the AU-rich region significantly enhanced the asynchronous deadenylation and overall decay rate. All three AREs carrying the 54-nt AU-rich region now directed a rapid decay with a pattern similar to that of the GM-CSF or IL-3 ARE. Together, these results showed that an AU-rich region 5′ to a cluster of AUUUA motifs is necessary to form a potent class II ARE.

A 5′ AU-rich region and a 3′ cluster of five AUUUA sequences are the critical features of a class II ARE. While the overlapping nonamers appear not to be the feature recognized by the decay machinery, are they sufficient to direct rapid decay of β-globin mRNA observed for both class I and class II AREs? A 18-nt ARE sequence bearing three overlapping nonamers, $UU(AUUU)_3AUU$ (Fig. 1 and Fig. 7, syn1 ARE), was synthesized and inserted into the β-globin 3′ UTR. Much to our surprise, the syn1 ARE had only a very modest destabilizing effect (Fig. 7). The β-globin messages bearing syn1 ARE underwent slow and highly synchronous deadenylation till the poly(A) tails were nearly removed by the 6-h time point. The deadenylated mRNAs were then gradually degraded with first-order kinetics. This result demonstrated that although the three overlapping nonamers were able to show some modest destabilizing effect, they were clearly not sufficient to direct rapid deadenylation and mRNA degradation observed for either the class I or II AUUUA-containing ARE.

The importance of a 5′ AU-rich region to the AUUUA cluster (Fig. 6) raised the possibility that the 54-nt AU-rich region may be able to potentiate the syn1 ARE to display the class II destabilizing power. Therefore, syn2 was created by fusing the 54-nt AU-rich region 5′ to syn1. The result in Fig. 7 showed that although the syn2 ARE becomes much more potent than the syn1 ARE, it does not possess the class II potency. β-Globin mRNAs bearing the syn2 ARE display highly synchronous deadenylation followed by decay of the RNA body, which is now similar to that of the c-*fos* class I ARE. Thus, these results provide further evidence to support that view that the 5′ AU-rich region is an integral part of a potent ARE. Our data show that a 5′ AU-rich region and a cluster of three AUUUA motifs are not sufficient to specify a class II ARE. Instead, the 5′ AU-rich region and five or six copies of AUUUA motifs clustered together may be sufficient.

To further address this issue, we introduced a double-point mutation to knock out the two AUUUA motifs in the 5′ region of the GM-CSF ARE to generate GM5. This mutant now has a 5′ AU-rich region without any AUUUA motifs plus a 3′ cluster of 5 AUUUA motifs, instead of 3 AUUUA motifs in the syn2 ARE. As shown in Fig. 7, β-globin mRNAs bearing

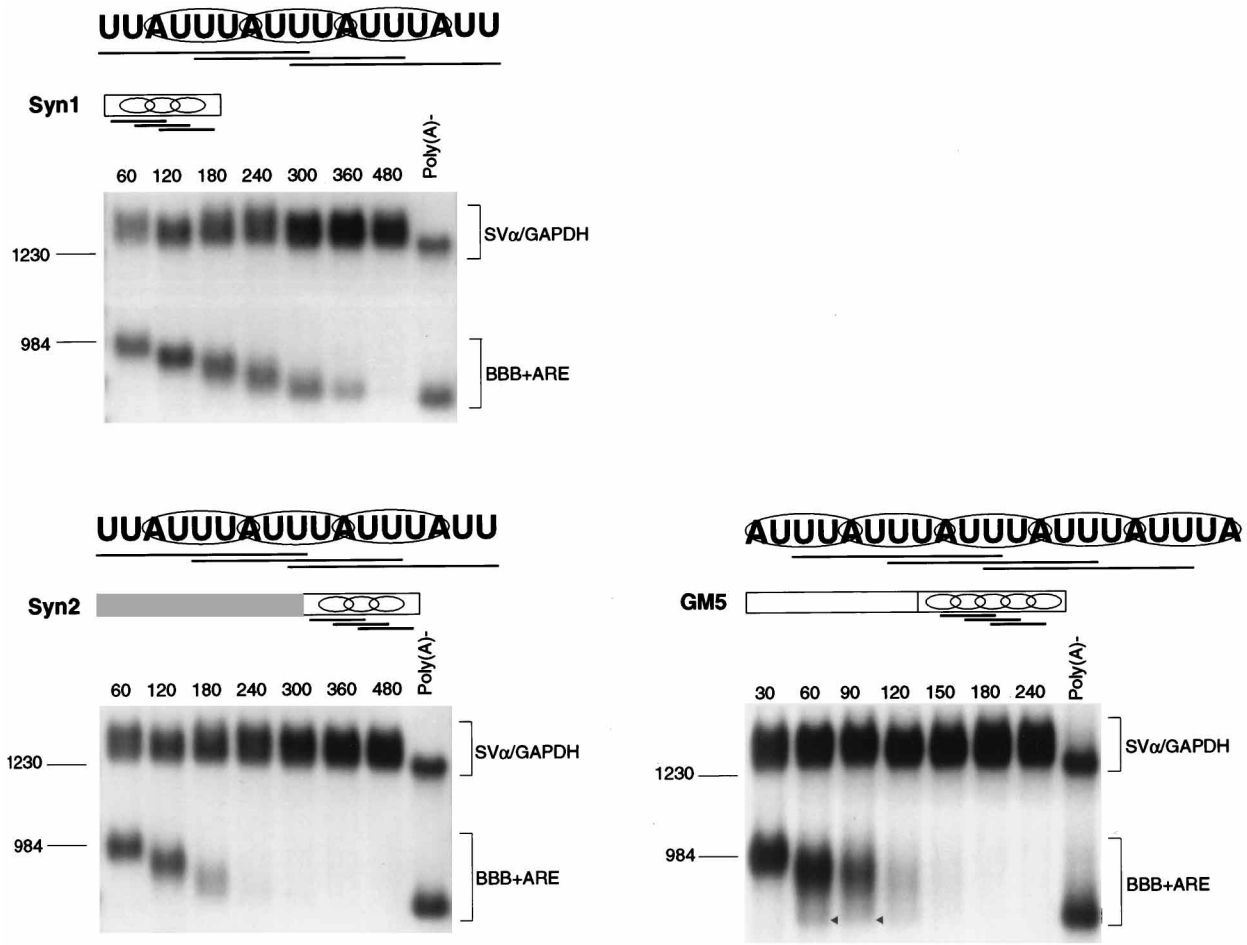

FIG. 7. A 5′ AU-rich region and a cluster of five AUUUA motifs are sufficient to generate a class II ARE. The schematic drawings of AREs, transient transfection, RNA isolation, and time course experiments are as described in the legend to Fig. 3. Northern blots show the decay of β-globin mRNAs containing the syn1, syn2, or GM5 ARE. Sequences of the cluster of AUUUA motifs or overlapping nonamers are shown over the blots.

this ARE were deadenylated and degraded with kinetics indistinguishable from those of the wt GM-CSF ARE. The results strongly support the view that an AU-rich region 5′ to a cluster of five or six AUUUA motifs is critical for a class II ARE to function. Moreover, the result also demonstrated that the two AUUUA motifs at the 5′ portion of the GM-CSF ARE are dispensable.

DISCUSSION

It has been a decade since the report of AU-rich sequence by Caput et al. (4) and subsequent demonstration by Shaw and Kamen (25) that an AU-rich sequence from the 3′ UTR of GM-CSF mRNA can function to destabilize a heterologous stable mRNA. Our understanding of the mechanisms by which AREs, the most common RNA-destabilizing elements among those characterized in mammalian cells, mediate mRNA turnover is still far from complete. This is due in part to a lack of a clear understanding of key sequence and structural features that dictate the destabilizing function of an ARE. As different AREs vary considerably in their size, AU content, and number of the AUUUA motif, it is not clear which features represent functionally critical elements (for a review, see reference 7). Moreover, the lack of any significant sequence homology among different AREs has further complicated the issue.

In an effort to define the general principles that govern the ARE-mediated decay, we and others have previously characterized the destabilizing function of a broad array of AREs and their mutant derivatives (e.g., 2, 5, 6, 8, 15, 22, 29, 31, 33). A few important points can be made concerning our methodology for monitoring mRNA turnover and decay kinetics. First, all the experiments were carried out without using transcription inhibitors, which have been shown to greatly affect ARE-mediated mRNA decay (8, 22). Second, changes in mRNA stability and decay kinetics were determined by performing rigorous time course experiments with an internal control message rather than solely determining the steady-state level of mRNA from a single time point. Third, since deadenylation is now recognized as the first step not only in ARE-directed mRNA degradation but also in the decay of many eukaryotic mRNAs (3, 6, 9, 14, 18), our system has offered thus far the unique opportunity to investigate this critical step in mammalian cells.

In this study, our experiments offer several new insights into the critical sequence features of AREs that govern the ARE-mediated mRNA degradation. Moreover, they provide further corroborating evidence that augments our previous classification of AREs (7, 22). First, a cluster of five or six copies of AUUUA motifs in close proximity with at least two of them being reiterated is the key feature that dictates the choice

between processive versus distributive deadenylation kinetics (Fig. 2). This feature is a common characteristic of class II AREs, e.g., GM-CSF, IL-3, and TNF-α AREs. Second, the clustering of AUUUA motifs, rather than the overlapping of nonamers that occurs concomitantly, represents the sequence entity that is recognized by the decay machinery. Neither overlapping nonamers nor the nonamer alone is able to confer significant destabilizing ability. Third, an AU-rich region 20 to 30 nt long immediately 5′ to this cluster of AUUUA motifs can greatly enhance the destabilizing ability of the AUUUA cluster and is, therefore, considered to be an integral part of an ARE.

A general picture emerges from our experiments and those of others. There appears to be a sequence hierarchy by which the three classes of AREs are composed from several key sequence features. The class III non-AUUUA ARE is a composite of a couple of U stretches and a U-rich domain. The appearance of one to three copies of the AUUUA motif in the context of an AU-rich region constitutes the class I AUUUA-containing ARE. Both classes direct deadenylation with distributive kinetics and reduce the half-life of β-globin mRNA down to ~35 min. The further addition of a few extra AUUUA motifs that introduce a cluster of five or six copies of the AUUUA motif at the 3′ portion of an ARE together with its 5′ AU-rich region generates the class II AUUUA-containing ARE. How might the destabilizing function of class II ARE be specified? It is the interplay of the 5′ AU-rich region and the 3′ cluster of AUUUA motifs that specifies the ultimate rapid and processive digestion of poly(A) tails. Since no significant sequence homology among those functional 5′ AU-rich regions in GM-CSF and IL-3, as well as the 54-nt sequence from the c-*fos* 3′ UTR, can be identified, there appears to be no stringent sequence requirements for both sequence features. We suspect that initial recognition of the 5′ AU-rich region by an ARE-binding protein might help to recruit and subsequently stabilize an mRNA-ribonucleoprotein complex that forms on the AUUUA cluster to invoke mRNA destabilization.

Zubiaga et al. (33) have reported that the nonamer UUA UUUAUU alone is sufficient to exhibit destabilizing ability and is thus the minimal functional ARE. It should be pointed out that the various synthetic AU-rich sequences they tested were all inserted immediately downstream of the 54-nt AU-rich sequence, which was assumed to have no enhancing effect on the destabilizing function of the tested AU-rich or nonamer sequences (33). When we tested the three overlapping nonamers in the absence of the 54-nt AU-rich sequence (syn1 ARE [Fig. 7]), no significant destabilizing effect could be detected. It took 4.5 h for the β-globin mRNA bearing this element to lose its poly(A) tail via distributive kinetics and then the RNA body was degraded with a half-life of more than 1 h. Conversely, in the case of class I ARE, 1 to 2 h is sufficient for the ARE to mediate removal of the poly(A) tail, which is followed by decay of RNA body with a half-life of 10 to 15 min. The class II AREs, e.g., the GM-CSF ARE, direct even faster removal of poly(A) with processive kinetics in less than 10 min. The RNA body is then degraded with a half-life of 10 to 15 min. Thus, in syn1 ARE-mediated decay, these two processes are considerably slower than those seen in either class I or class II AREs. This observation is consistent with the study by Lagnado et al. showing that even the most potent destabilizing sequence bearing three nonamers (ARE7 [15]) has only a modest destabilizing ability, similar to that of the syn1 ARE. Taken together, these observations support our notion that the interplay among AUUUA motifs, AU richness, and U stretches determines the ultimate destabilizing function of an ARE.

Our results are consistent with the interpretation that the nonamer UUAUUUA(U/A)(U/A) is not an essential sequence motif of AREs. It should be noted that there are two classes of AREs, class I and class III, that do not carry the nonamer yet have a potent destabilizing function. Single- or double-point mutations that knock out the only copy of the nonamer found in the c-*fos* ARE have no effect on its RNA-destabilizing ability (5). A few class III non-AUUA AREs, native or synthetic, that do not bear any copy of the AUUUA motif or nonamer still display a powerful RNA-destabilizing ability which is comparable to that of the c-*fos* ARE (22). Therefore, these observations demonstrate that the presence of a nonamer(s) is not an absolute requirement for AREs to be able to function as a potent RNA destabilizing element. Moreover, our mutagenesis study of the GM-CSF AREs (GM0, GM1, GM2, and GM3) rule out this precise nonameric consensus sequence as being a key sequence feature for the class II AUUUA-containing ARE. When comparing the syn2 ARE with the GM5 ARE, it is clear that although they all share a similar sequence backbone, a 5′ AU-rich region plus a 3′ cluster of AUUUA motifs, the GM5 ARE, which contains five reiterating AUUUA motifs, is much more potent than the syn2 ARE, which has three AUUUA motifs in the 3′ AUUUA cluster (Fig. 7). Taken together, we conclude that the AUUUA motif and not the nonamer, is the minimal sequence motif of AREs. The nonamer with the AUUUA core may be the smallest ARE that can exert modest destabilizing function in conjunction with an 5′ AU-rich region.

Finally, the results of our experiments provide circumstantial evidence to support the existence of cross talk between the ARE and the 3′ end poly(A) tail, which dictates the rate and kinetics of cytoplasmic deadenylation and thereby the fate of the corresponding mRNA. One of the possibilities is that an ARE-binding protein or a complex interacts concurrently with an ARE in the 3′ UTR and poly(A) tail at the 3′ end associated with poly(A)-binding proteins. Depending on the ARE sequence and its cognate binding protein, this interaction might determine the kinetics and rate of poly(A) tail removal and thereby lead to subsequent degradation of the message body, e.g., by decapping followed by 5′-to-3′ exonuclease digestion. Alternatively, an ARE-binding protein or a complex might stabilize mRNA through its simultaneous association with both the ARE and the poly(A) tail. A recent report by Abe et al. (1) provided evidence supporting such an interaction. They showed that mouse HuC, an ARE-binding protein suggested to play important roles in neuronal differentiation and maintenance, displays specific RNA binding activity both for the ARE and the poly(A) sequence. Whether modulation of the level of HuC proteins may affect the ARE-directed mRNA decay and in what direction await further experimentation. One of the pressing issues will be to determine whether and how the various ARE-binding proteins identified thus far (11, 16, 17, 19, 20, 21, 32) affect the deadenylation and decay kinetics displayed by different classes of AREs. Our studies of the sequence features of AREs and the respective deadenylation and decay kinetics will provide the groundwork for future characterization of ARE-binding proteins identified by in vitro gel shift assays in order to stringently define their participation in ARE-mediated mRNA degradation.

ACKNOWLEDGMENTS

We thank Julia Lever for critical reading of the manuscript and valuable comments.

This work was supported by NIH grant GM-46454 and in part by a grant from the Council of Tobacco Research-USA, Inc. A.-B. S. is the recipient of an American Heart Association Established Investigator

Award. C.-Y. A. C. is the recipient of a Research Planning Award from the National Science Foundation.

REFERENCES

1. **Abe, R., E. Sakashita, K. Yamamoto, and H. Sakamoto.** 1996. Two different RNA binding activities for the AU-rich element and the poly(A) sequence of the mouse neuronal protein mHuC. Nucleic Acids Res. **24:**4895–4901.
2. **Akashi, M., G. Shaw, M. Gross, M. Saito, and P. Koeffler.** 1991. Role of AUUU sequences in stabilization of granulocyte-macrophage colony-stimulating factor RNA in stimulated cells. Blood **78:**2005–2012.
3. **Beelman, C. A., and R. Parker.** 1995. Degradation of mRNA in eukaryotes. Cell **81:**179–183.
4. **Caput, D., B. Beutler, K. Hartog, R. Thayer, S. Brown-Shimer, and A. Cerami.** 1986. Identification of a common nucleotide sequence in the 3′-untranslated regions of mRNA molecules specifying inflammatory mediators. Proc. Natl. Acad. Sci. USA **83:**1670–1674.
5. **Chen, C.-Y. A., T.-M. Chen, and A.-B. Shyu.** 1994. Interplay of two functionally and structurally distinct domains of the c-*fos* AU-rich element specifies its mRNA-destabilizing function. Mol. Cell. Biol. **14:**416–426.
6. **Chen, C.-Y. A. and A.-B. Shyu.** 1994. Selective degradation of early-response-gene mRNAs: functional analyses of sequence features of the AU-rich elements. Mol. Cell. Biol. **14:**8471–8482.
7. **Chen, C.-Y. A., and A.-B. Shyu.** 1995. AU-rich elements: characterization and importance in mRNA degradation. Trends Biochem. Sci. **20:**465–470.
8. **Chen, C.-Y. A., N. Xu, and A.-B. Shyu.** 1995. mRNA decay mediated by two distinct AU-rich elements from c-*fos* and GM-CSF transcripts: different deadenylation kinetics and uncoupling from translation. Mol. Cell. Biol. **15:**5777–5788.
9. **Decker, C. J., and R. Parker.** 1993. A turnover pathway for both stable and unstable mRNAs in yeast: evidence for a requirement for deadenylation. Genes Dev. **7:**1632–1643.
10. **Greenberg, M. E., and E. Ziff.** 1984. Stimulation of 3T3 cells induces transcription of the c-*fos* proto-oncogene. Nature (London) **311:**433–438.
11. **Hamilton, B. J., E. Nagy, J. S. Malter, B. A. Arrick, and W. F. Rigby.** 1993. Association of heterogeneous nuclear ribonucleoprotein A1 and C proteins with reiterated AUUUA sequences. J. Biol. Chem. **268:**8881–8887.
12. **Higuchi, R.** 1990. Recombinant PCR, p. 177–183. *In* M. A. Innis, D. H. Gelfand, J. J. Sninsky, and T. J. White (ed.), PCR protocols: a guide to methods and applications. Academic Press, San Diego, Calif.
13. **Jacobson, A., and S. W. Peltz.** 1996. Interrelationships of the pathways of mRNA decay and translation in eukaryotic cells. Annu. Rev. Biochem. **65:** 693–740.
14. **Jacobson, A.** 1996. Poly(A) metabolism and translation: the closed loop model, p. 451–480. *In* J. Hershey, M. Mathews, and N. Sonenberg (ed.), Translational control. Cold Spring Harbor Press, New York, N.Y.
15. **Lagnado, C. A., C. Y. Brown, and G. J. Goodall.** 1994. AUUUA is not sufficient to promote poly(A) shortening and degradation of an mRNA: the functional sequence within AU-rich elements may be UUAUUUA(U/A)(U/A). Mol. Cell. Biol. **14:**7984–7995.
16. **Levine, T. D., F. Gao, P. H. King, L. G. Andrews, and J. D. Keene.** 1993. Hel-N1: an autoimmune RNA-binding protein with specificity for 3′ uridylate-rich untranslated regions of growth factor mRNAs. Mol. Cell. Biol. **13:**3494–3504.
17. **Ma, W.-J., S. Cheng, A. Wright, C. Campbell, and H. M. Furneaux.** 1996. Cloning and characterization of HuR, a ubiquitously expressed Elav-like protein. J. Biol. Chem. **271:**8144–8151.
18. **Muhlrad, D., and R. Parker.** 1994. Deadenylation of the unstable mRNA encoded by the yeast *MFA2* gene leads to decapping followed by 5′→3′ digestion of the transcript. Genes Dev. **8:**855–866.
19. **Nagy, E., and W. F. C. Rigby.** 1995. Glyceraldehyde-3-phosphate dehydrogenase selectively binds AU-rich RNA in the NAD^+-binding region (Rossmann fold). J. Biol. Chem. **270:**2755–2763.
20. **Nakagawa, J., H. Waldner, S. Meyer-Monard, J. Hofsteenge, P. Jenö, and C. Moroni.** 1995. AUH, a novel gene encoding an AU-specific RNA binding protein with intrinsic enoyl-CoA hydratase activity. Proc. Natl. Acad. Sci. USA **92:**2051–2055.
21. **Nanbu, R., T. Kubo, T. Hashimoto, and S. Natori.** 1993. Purification of an AU-rich RNA binding protein from Sarcophaga peregrina (flesh fly) and its identification as a thiolase. J. Biochem. **114:**432–437.
22. **Peng, S. S.-Y., C.-Y. A. Chen, and A.-B. Shyu.** 1996. Functional characterization of a non-AUUUA AU-rich element from the c-*jun* proto-oncogene mRNA: evidence for a novel class of AU-rich elements. Mol. Cell. Biol. **16:**1490–1499.
23. **Richter, J. D.** 1996. Dynamics of poly(A) addition and removal during development, p. 481–504. *In* J. Hershey, M. Mathews, and N. Sonenberg (ed.), Translational control. Cold Spring Harbor Press, New York, N.Y.
24. **Ross, J.** 1995. mRNA stability in mammalian cells. Microbiol. Rev. **59:**16–95.
25. **Shaw, G., and R. Kamen.** 1986. A conserved AU sequence from the 3′ untranslated region of GM-CSF mRNA mediates selective mRNA degradation. Cell **46:**659–667.
26. **Shyu, A.-B., J. G. Belasco, and M. E. Greenberg.** 1991. Two distinct destabilizing elements in the c-*fos* message trigger deadenylation as a first step in rapid mRNA decay. Genes Dev. **5:**221–231.
27. **Shyu, A.-B., J. A. Garcia-Sanz, and E. Mullner.** 1996. Analysis of mRNA decay in mammalian cells, p. 449–456. *In* I. Lefkovits (ed.), The immunology methods manual. Academic Press, London, United Kingdom.
28. **Shyu, A.-B., M. E. Greenberg, and J. G. Belasco.** 1989. The c-*fos* transcript is targeted for rapid decay by two distinct mRNA degradation pathways. Genes Dev. **3:**60–72.
29. **Stoecklin, G., S. Hahn, and C. Moroni.** 1994. Functional hierarchy of AUUUA motifs in mediating rapid interleukin-3 mRNA decay. J. Biol. Chem. **269:**28591–28597.
30. **Treisman, R.** 1985. Transient accumulation of c-*fos* RNA following serum stimulation requires a conserved 5′ element and c-*fos* 3′ sequence. Cell **42:**889–902.
31. **Wilson, T., and R. Treisman.** 1988. Removal of poly(A) tail and consequent degradation of c-*fos* mRNA facilitated by 3′ AU-rich sequence. Nature (London) **366:**396–399.
32. **Zhang, W., B. J. Wagner, K. Ehrenman, A. W. Schaefer, C. T. DeMaria, D. Crater, K. DeHaven, L. Long, and G. Brewer.** 1993. Purification, characterization, and cDNA cloning of an AU-rich element RNA-binding protein, AUF1. Mol. Cell. Biol. **13:**7652–7665.
33. **Zubiaga, A. M., J. G. Belasco, and M. E. Greenberg.** 1995. The nonamer UUAUUUAUU is the key AU-rich sequence motif that mediates mRNA degradation. Mol. Cell. Biol. **15:**2219–2230.